ELSEVIER

Journal of Photochemistry and Photobiology A: Chemistry 99 (1996) 145–153

Journal of PHOTOCHEMISTRY AND PHOTOBIOLOGY A:CHEMISTRY

Dynamics of light-induced excited state quenching of ferrioxalate complexes by peroxides. Fast kinetic events and interaction with toxic pollutants

V. Nadtochenko [1], J. Kiwi

Institute of Physical Chemistry II, Swiss Federal Institute of Technology, 1015 Lausanne, Switzerland

Received 23 February 1996; accepted 17 April 1996

Abstract

The behaviour of the trioxaloferrate ($Fe(ox)_3^{3-}$) complex on laser illumination and its quenching in the presence of H_2O_2 were investigated by laser photolysis. At neutral Ph, a short (approximately 30 μs) and a longer (approximately 1 ms) lifetime were observed for transient $Fe(ox)_3^{3-}$. The lifetime decreases as the pH becomes more acidic. In light-induced processes, the intensity of the light used is one of the determining reaction parameters and this effect is reported in detail. The excited states of the Fe oxalate complexes induced by laser photolysis are quenched by H_2O_2. The decay observed can be fitted in a simplified way by a bi-exponential function. The transient species $Fe(ox)_3^{3-*}$ observed on laser photolysis does not undergo excited state annihilation, but ground state collisional quenching. The fast formation of a hydroxylated phenol adduct is shown by kinetic laser spectroscopy. A detailed account of the kinetics and spectral characteristics of the transients is presented for these reactions. This allows a scheme to be suggested for the intervention of these radicals in agreement with the experimental observations. The results obtained implicate the $^{\bullet}OH$ radical in the degradation of pollutants involving Fe complexes in the presence of H_2O_2.

Keywords: Adduct formation; Fast kinetics; Fe oxalate; Laser photolysis; $^{\bullet}OH$ radicals; Peroxides; Phenol; Quenching of complexes

1. Introduction

In the period between 1910 and 1950, the photochemical behaviour of trioxaloferrate ($Fe(ox)_3^{3-}$) was studied by a number of workers. The main results have been compiled in recent reviews [1–4]. The absorption and intensity of the continuous band extending from 200 to 550 nm depends on the acidity of the solution and the oxalate/Fe^{III} ratio. Most of the published work suggests that there is an equilibrium between the monooxalate, bioxalate and trioxalate complexes. Work has been carried out recently [5–12] on this complex via flash photolysis [12], stop flow and steady state irradiation within the millisecond, second and longer timescales respectively. In this work, we study this system over a much shorter time region (nanosecond region onwards) via ruby laser-pulsed photolysis. The conditions used are such that the tris complex is the only significant species present in acidic media. The characteristics of $Fe(ox)_3^{3-}$ decay in the absence and presence of H_2O_2 during photodriven laser-induced reactions are the main objective of this study. The fast laser pulse (15 ns) allows a suitable observation of the lifetime of the ligand to metal charge transfer (LMCT) of the excited complex. The kinetic features of the excited species were investigated under various conditions. The fast kinetics associated with the photoreduction of Fe^{III} oxalate in dilute solution (not reported until now) were explored during the course of this study.

Many workers regard Fenton chemistry as the production of $^{\bullet}OH$ radicals from iron–H_2O_2–UV or dark reactions [13–17]. However, recent work [4,13] has shown that the rate of photolytic destruction of H_2O_2 is accelerated in the presence of ferrioxalate. This lends further support to the importance of the study presented here. This latter observation has important implications in the destruction of organic pollutants, such as phenol, in industrial waste waters. Therefore we investigated the fast kinetics associated with the $^{\bullet}OH$ adduct through the laser-induced reactions of the $Fe(ox)_3^{3-}$–H_2O_2–phenol–UV system. This approach seems promising for the degradation of organic pollutants because it allows longer wavelengths to be used than classical Fenton systems. This has

[1] Visiting scientist: Institute of Physical Chemistry, Russian Academy of Sciences, Chernogolovka 142432, Moscow Region, Russia.

PII S1010-6030(96)04377-8

important consequences regarding solar energy utilization when activating these reactions.

2. Experimental section

2.1. Materials employed

$FeCl_3$, dihydrooxalic acid, sodium oxalate, potassium oxalate, phenol and H_2O were Fluka p.a. products and were used as received. $Fe(ox)_3^{3-}$ was prepared by different methods by a suitable combination of adequate reagents, and no differences were observed in the final product as a function of the preparation procedure.

2.2. Laser photolysis

Laser photolysis was carried out using the second harmonic ($\lambda = 347$ nm) of a JK-2000 ruby laser operated in the Q-switched mode. The pulse width was about 15 ns and the energy per pulse was approximately 10 mJ. The laser pulse energy was monitored and the experimental results were normalized according to these measured energies. The mean average of the laser beam diameter was 0.5 cm. The detection of the transient absorption changes was performed via an EGG photomultiplier with a rise time of about 5 ns. The preamplifier full bandwidth at 125 MHz was used to register the signals in the nanosecond region and up to 5 μs. At longer times, the bandwidth was narrowed to 5 MHz. The detection system used for kinetic spectroscopy has been reported previously [5]. All solutions were used only once to avoid accumulation of the irradiated products and the irreversible decomposition of the ferrioxalate by laser photolysis. The prevention of the decomposition of $Fe(ox)_3^{3-}$ was achieved in two ways: (1) the solutions were stored in the dark before use; (2) the monitoring Xe light used for the detection of the intermediates was narrowed by Schott SKF bandpass filters. These filters allowed light to pass in the region of $\Delta\lambda \cong 20$ nm and were centred each time at the appropriate λ of interest. All experiments were performed in 1 cm quartz cells in aerated solutions at room temperature.

Spectrophotometric analysis of the absorbance of the solution used to generate the $Fe(ox)_3^{3-}$ transient by laser photolysis was carried out using a Hewlett Packard 8452 diode array. The decomposition was observed in all cases to be less than 5% when H_2O_2 was mixed with $Fe(ox)_3^{3-}$ immediately before use.

3. Results and discussion

3.1. Monophotonic character of the laser-induced photolysis of ferrioxalate $Fe(ox)_3^{3-}$ and biexponential decay of the observed intermediates

The photochemistry of the ferrioxalate actinometer has been extensively studied, but with a much lower time resolution. Three oxalate complexes of Fe^{III} have been reported to exist in solution, all with high stability constants: (1) monooxalate with $k_1 = 5.5 \times 10^7$ (mol l^{-1})$^{-1}$ [6,7]; (2) dioxalate with $k_2 = 10^{14.6}$ (mol l^{-1})$^{-1}$ [8]; (3) $Fe(ox)_3^{3-}$ with $k_3 = 10^{20}$ (mol l^{-1})$^{-1}$ [9]. Fig. 1 shows the linear dependence of the changes in the amplitude of the optical density (ΔOD) during laser-induced photolysis of ferrioxalate $Fe(ox)_3^{3-}$ at $\lambda = 400$ nm. The solution used in Fig. 1 contained Fe^{III} (0.57 mmol l^{-1}) and oxalate (4.13 mmol l^{-1}). The graph in Fig. 1 shows a linear dependence indicating that there is a one-photon photoresponse to the light intensity. The highest ΔOD of around 0.06 corresponds to 10 mJ per pulse. The amplitude changes by a factor of eight. The exponential nature of the decay is substantiated by the fact that the different decay curves intersect at only one point in the time domain (see inset) for different initial amplitudes or applied pulse energies. This experimental observation allows us to discard the possibility of second-order reactions, such as quenching between excited states and dismutation of oxalic radicals. These results extend work carried out previously by flash photolysis with a slower time resolution [6,9,13]. Fig. 2(a) reports the changes in the optical density as a function of time for different concentrations of oxalate but keeping the Fe^{III} concentration at 0.57 mmol l^{-1}. A well-defined two-component decay is observed in Fig. 2(a) with fast (approximately 50 μs) and slow (millisecond range) components. For oxalate concentrations of 1.25, 4.13 and 18 mmol l^{-1}, the lifetimes of the fast components are 29, 21 and 17 μs and those of the long-lived components are 0.5, 1.5 and 2.3 ms respectively.

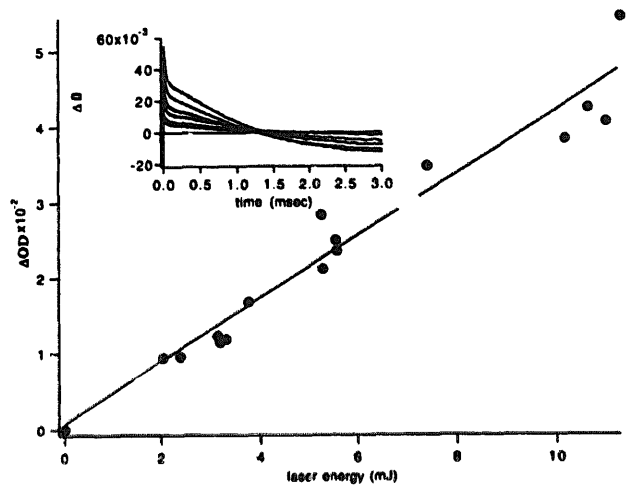

Fig. 1. Differential absorption of a solution of Fe^{III} (0.6 mmol l^{-1}) and oxalate (4.13 mmol l^{-1}) at $\lambda = 400$ nm and 2 μs after the laser pulse vs. the laser pulse energy (mJ) (for other details and inset, see text).

The changes in the form of the transient as a function of concentration are attributed to the variation in the complex composition $Fe(ox)_n^{3-2n}$ where $n = 1$, 2 or 3. The higher oxalate concentrations in Fig. 2(a) involve preferentially the tris-oxalate complex and this is the case for an oxalate concentration of 4 mmol l^{-1}. For this reason, the transient decay rate was found to be dependent on the oxalate concentration.

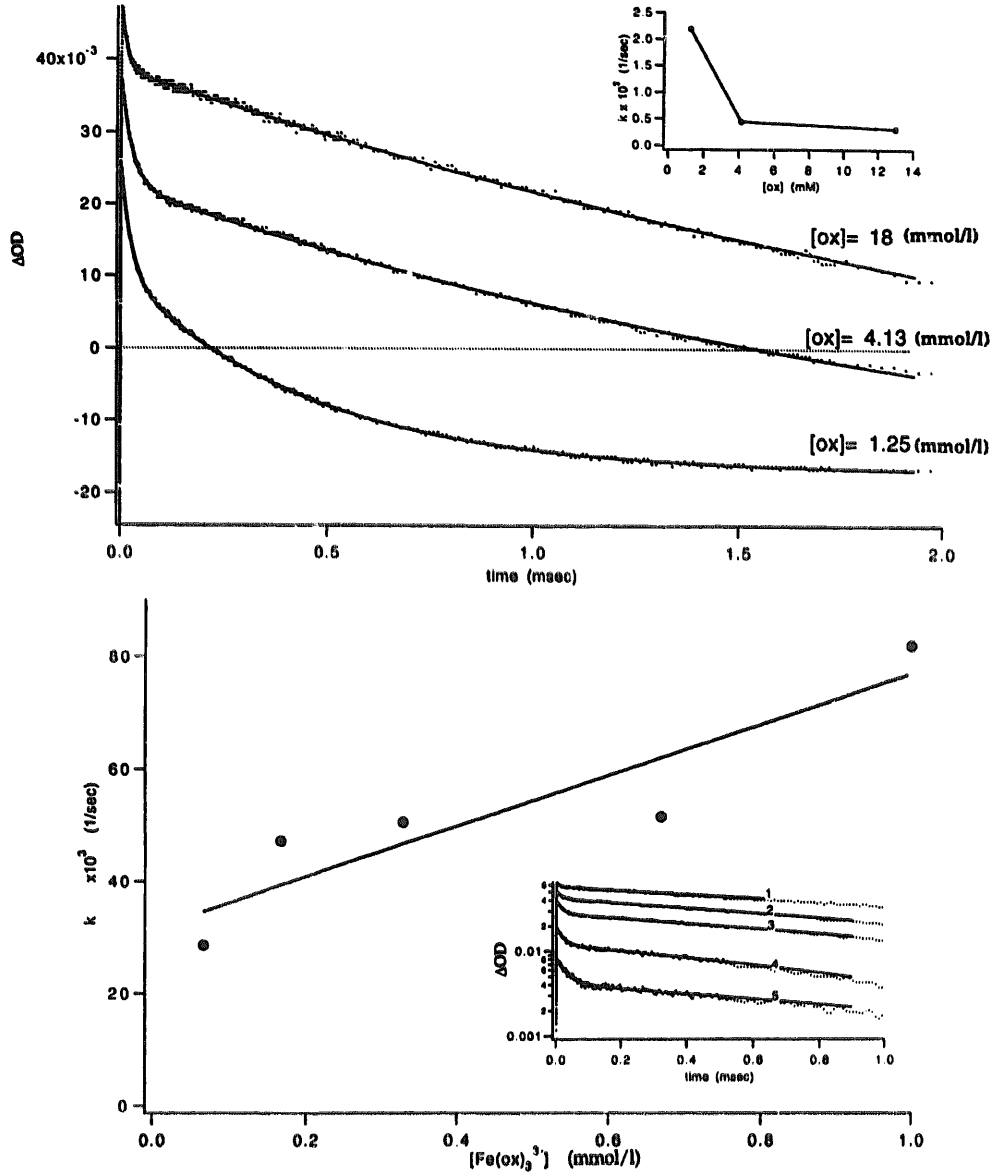

Fig. 2. (a) Differential optical absorption of a solution of Fe^{III} (0.57 mmol l^{-1}) at different oxalate concentrations vs. the time after the laser pulse. (b) Rate constant vs. concentration of the complex at a constant oxalate/Fe^{III} ratio of 21 and pH 6.5. The traces in the insert were carried out at Fe oxalate concentrations of 1 mmol l^{-1} (1), 0.67 mmol l^{-1} (2), 0.33 mmol l^{-1} (3), 0.17 mmol l^{-1} (4) and 0.07 mmol l^{-1} (5).

Fig. 2(b) shows the transient curves at different Fe oxalate concentrations of 0.07 mmol l^{-1} (trace 5) up to 1 mmol l^{-1} (trace 1), but conserving the ratio of Fe^{III}/(oxalate) = 21 at pH 6.5. On going from the lower $Fe(ox)_3^{3-}$ concentration to the higher concentration, a reduction in the lifetime of the fast component is observed. The long-lived component in Fig. 2(b) does not vary with concentration in the experimental range investigated. From Stern–Volmer plots obtained for the fast component (reciprocal lifetime vs. the concentration of $Fe(ox)_3^{3-}$), a lifetime of 31 ± 5 μs in the limit of zero Fe oxalate concentration is obtained for the fast component decay. The rate constant for excited $Fe(ox)_3^{3-}$* quenching by an equivalent non-excited complex is $(4.5 \pm 1.2) \times 10^7$ (mol l^{-1})$^{-1}$ s^{-1} in Fig. 2(b). The two-component decay in Fig. 2 can be ascribed to $Fe(ox)_3^{3-}$, an LMCT complex and intermediates such as $[(ox)_2Fe(ox^{\cdot -})]^{3-}$ and possibly other species [6–14].

3.2. Laser studies of the kinetics of the excited state of $Fe(ox)_3^{3-}$ as a function of the pH of the solution

Fig. 3 presents the results of laser flash photolysis for solutions containing Fe^{III} (0.6 mmol l^{-1}) and sodium oxalate (18 mmol l^{-1}) at different pH values. The inset in Fig. 3(a) shows the decay in the microsecond range of the transient at $\lambda = 400$ nm. The inset in Fig. 3(b) shows the decay in the millisecond time domain. The dependence of the reciprocal lifetime k (s^{-1}) on the pH in Fig. 3(a) shows that a shortening of the lifetime occurs for the fast component of the decay. For the fast component, the observed decay rate

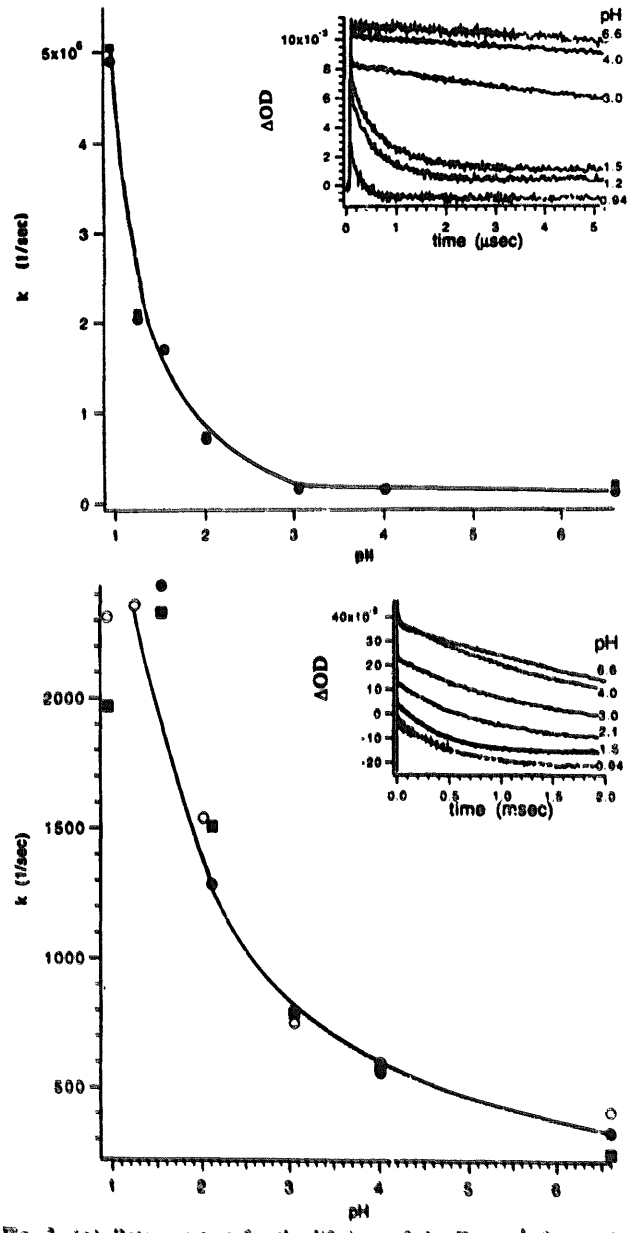

Fig. 3. (a) Rate constant for the lifetime of the $Fe(ox)_3^{3-}$* complex (Fe^{III} = 0.6 mmol l^{-1} and oxalate = 18 mmol l^{-1}) as a function of pH in the microsecond region after the laser pulse. (b) Rate constant vs. pH for the same solution as reported in (a) but in the millisecond domain.

changes by a factor of about 50 on going from pH 0.9 to neutral pH 6.6.

Fig. 3(b) shows the decay time for the long-lived component vs. pH for the same solution as in Fig. 3(a), but in the millisecond range. The decay rate in Fig. 3(b) changes by a factor of about five on going from acid to neutral pH. A more pronounced bleaching effect for the laser signals is observed at acidic pH values. The changes observed in the lifetime and form of the transient decay (see inset) reflect the presence of excited and non-excited species with changing composition as a function of the pH of the medium. The interaction of Fe complex excited states with H^+ [6,16–18] and other reactions, such as aquation and equilibration [7,12], are occurring. They have been reported for $Fe(ox)_3^{3-}$ complexes.

3.3. Differential transient absorption spectra during $Fe(ox)_3^{3-}$ photolysis

The differential spectra for a solution of Fe^{III} (0.6 mmol l^{-1}) and oxalate (18 mmol l^{-1}) at pH 6.6 and 1.1 are shown in Fig. 4(a) and 4(b) respectively. The insets in these two figures show the transient decay at the maximum for the differential optical spectra (approximately 400 nm). The decay transients are similar for different λ up to the millisecond range in aerated solutions.

The maximum in Fig. 4(a) and 4(b) shifts with time to longer λ. The decay observed for $Fe(ox)_3^{3-}$* and the growing in of the $[(ox)_2Fe(ox^{\cdot-})]$ signal cause the shift observed in the differential spectra. The absorption coefficient of $Fe(ox)_3^{3-}$* is therefore higher than that of $[(ox)_2Fe(ox^{\cdot-})]$. Negative absorption predominates below λ = 380 nm due to ground state bleaching, indicating that the extinction coefficients of the ground state complexes are larger than those of the excited states.

Fig. 4(b) shows the transient spectra for the same solution as used in Fig. 4(a), but at acidic pH (1.05). The times of the spectral observations after the laser pulse are indicated in Fig. 4(b) between 5 μs and 2 ms. Between the λ values of

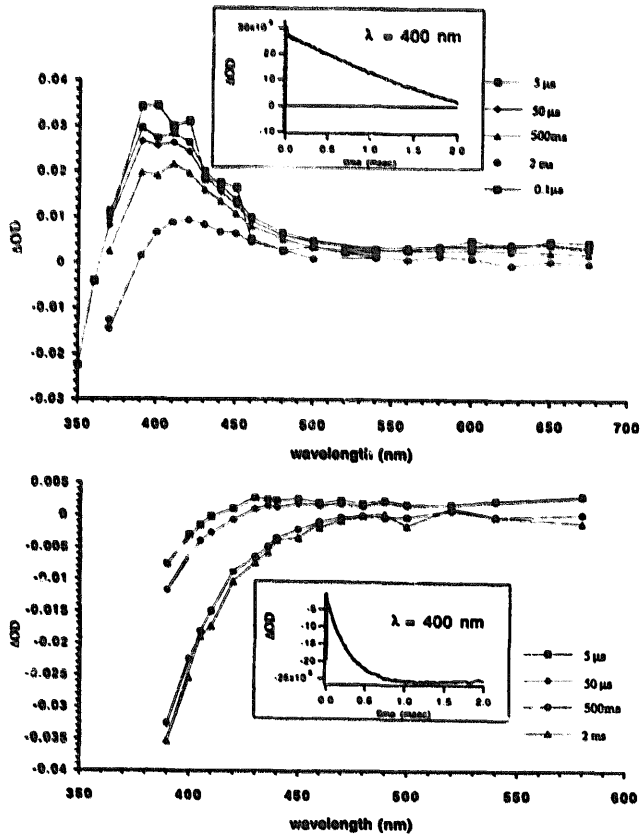

Fig. 4. (a) Transient decay spectra for $Fe(ox)_3^{3-}$* (Fe^{III} = 0.6 mmol l^{-1} and oxalate = 18 mmol l^{-1}; pH 6.5) as a function of λ at the times noted. The inset at 400 nm shows the decay of the transient in the millisecond range. (b) The same spectra as in (a) but at a solution pH of 1.1.

380 and 580 nm, a significant change is observed in the optical differential spectrum, with no maximum and a stronger negative absorption as a function of λ in comparison with the spectrum reported in Fig. 4(a). This effect becomes more marked at longer times (2 ms). A lower pH decreases the complex absorption and shifts the bleaching to longer λ.

From the experimental observations presented in this study (Section 3.1Section 3.2Section 3.3Section 3.4, a kinetic scheme for the laser-induced reactions can be outlined

$$Fe^{III}(ox)_3^{3-} + h\nu \rightarrow Fe^{III}(ox)_3^{3-*} \quad (1)$$

$$Fe^{III}(ox)_3^{3-*} \rightarrow Fe^{III}(ox)_3^{3-} \quad k_2 \quad (2)$$

$$Fe^{III}(ox)_3^{3-*} \rightarrow Fe^{II}(ox)_2^{2-} + ox^{\cdot -} \quad k_3 \quad (3)$$

$$Fe(ox)_3^{3-*} + Fe(ox)_3^{3-} \rightarrow 2Fe(ox)_3^{3-} \quad k_4 \quad (4)$$

$$Fe(ox)_3^{3-} \longrightarrow \left[(C_2O_4)_2Fe\begin{smallmatrix}O-CO\\O-CO\end{smallmatrix}\right]^{3-} \quad k_5 \quad (5)$$

$$\left[(C_2O_4)_2Fe\begin{smallmatrix}O-CO\\O-CO\end{smallmatrix}\right]^{3-} (ox)_2Fe(ox^{\cdot -}) \longrightarrow Fe(ox)_2^{2-} + ox^{\cdot -} \quad k_6 \quad (6)$$

The formation of steady state photolysis products as reported by classical work [10–13] involves

$$ox^{\cdot -} + Fe(ox)_3^{3-} \rightarrow Fe(ox)_2^{2-} + ox^{2-} + 2CO_2 \quad k_7 \quad (7)$$

The integration of differential equations corresponding to reactions (2)–(7) involves a three-exponential decay

$$\Delta OD(t) = OD(Fe(ox)_3^{3-}) + OD(Fe(ox)_3^{3-*}) + OD((ox)_2Fe(ox^{\cdot -})) + OD(ox^{\cdot -}) + OD(Fe(ox)_2^{2-}) + OD(Fe(ox)_3^{3-})|t=0$$

$$\Delta OD(t) = A_0 + A_1 \exp(-t/T_1) + A_2 \exp(-t/T_2) + A_3 \exp(-t/T_3) \quad (8)$$

$$T_1 = 1/(k_1 + k_2 + k_3 + k_4[Fe(ox)_3^{3-}]) = 1/k_q \quad (9)$$

$$T_2 = 1/k_5 \quad (10)$$

$$T_3 = 1/k_7[Fe(ox)_3^{3-}]_0 \quad (11)$$

The amplitudes of the laser signals A_0, A_1, A_2 and A_3 and the observed transient lifetimes T_1, T_2 and T_3 on the right-hand side of Eq. (8) are a function of the rate constants k_2–k_7 and the initial concentrations of the Fe^{III} oxalate complexes in Eqs. (3)–(8) and $Fe(ox)_3^{3-*}$ at $t=0$. Since the extinction coefficients of $ox^{\cdot -}$, $(C_2O_4^{\cdot -})$, $CO_2^{\cdot -}$ and $Fe^{II}(ox)_2^{2-}$ below $\lambda = 360$ nm are negligible, it follows that the equations for the transients should be simplified to a bi-exponential representation. Evidence for this is given in Fig. 2. Eq. (8) will then become

$$\Delta OD(t) = A_0 + A_1 \exp(-t/T_1) + A_2 \exp(-t/T_2) \quad (12)$$

The experimental observation in Fig. 2(b) of the reverse proportionality between the rate constant involving T_1 and the initial ferrioxalate concentration in a Stern–Volmer plot is an important consequence of the suggested model.

The microsecond component in Fig. 2(a) represents the excited state in Eq. (1). The dependence in Fig. 2(b) of the lifetime of the excited intermediate on the oxalate concentration shows that Eq. (4) proceeds under the conditions used. The longer component of the decay in Figs. 2 and 3 in the millisecond range represents the metastable longer lived species $(ox)_2Fe(ox^{\cdot -})$ [10,11]. The absorption of photons (Eq. (1)) and the deactivation of the excited species occur in the microsecond range. The excited species transfers an electron from the ligand to the Fe^{III} ion producing an Fe^{II} ion and, subsequently, reaction (6) occurs with oxalate elimination. This process is suggested to occur in the nanosecond and microsecond range (the fast decay in the results presented).

3.4. Fast kinetics observed during the interaction of $Fe(ox)_3^{3-}$ with H_2O_2

Fig. 5(a) shows the interaction of $Fe(ox)_3^{3-}$ with H_2O_2 at three concentrations of the latter following initial laser excitation. The Fe^{III} and oxalate concentrations used were 0.6 mmol l^{-1} and 18 mmol l^{-1} respectively. A shortening of the lifetime of the excited species in Fig. 5 means that quenching is taking place due to H_2O_2, with the formation of transients and reaction products. For the slow and fast component decay of the excited state, the Stern–Volmer plot is valid, and the rate constants for the quenching of $Fe(ox)_3^{3-*}$ by H_2O_2 from Fig. 5(b) are close to $(2\pm0.2)\times10^5$ (mol $l^{-1})^{-1}$ s^{-1}. Other information involving the fast and slow components of the decay and the experimental conditions used is shown in Table 1. Dark reactions of metal–organic species complexes have been sparingly reported in the literature and present some of the known mechanistic features of the Fenton reagent [16,17].

The transient spectra at different times after the laser pulse for a solution of Fe^{III} (0.6 mmol l^{-1}), oxalate (18 mmol l^{-1}) and H_2O_2 (0.29 mol l^{-1}) at pH 6 are shown in Fig. 5(c). The inset in Fig. 5(c) shows the transient in a solution of $Fe(ox)_3^{3-*}$ in the presence of H_2O_2 (0.29 mol l^{-1}). This transient is quite different from the transient reported previously for this complex in the absence of the peroxide in the top trace of Fig. 2. The inset in Fig. 5(c) shows a shorter lifetime in the microsecond range for the $Fe(ox)_3^{3-*}$ excited state.

Fig. 5(d) shows the transient spectra for the same solution as used in Fig. 5(c), but at a solution pH of 1.05. The difference in the shape of the observed spectra reflects the different composition of the transient as a function of the solution pH. The inset in Fig. 5(d) shows the transient at $\lambda = 400$ nm with a lifetime of around 33 μs. The latter time is shorter than the value reported in the inset of Fig. 5(c) (pH 6.6), confirming the importance of the pH in the lifetime of the Fe oxalate excited state quenched by H_2O_2.

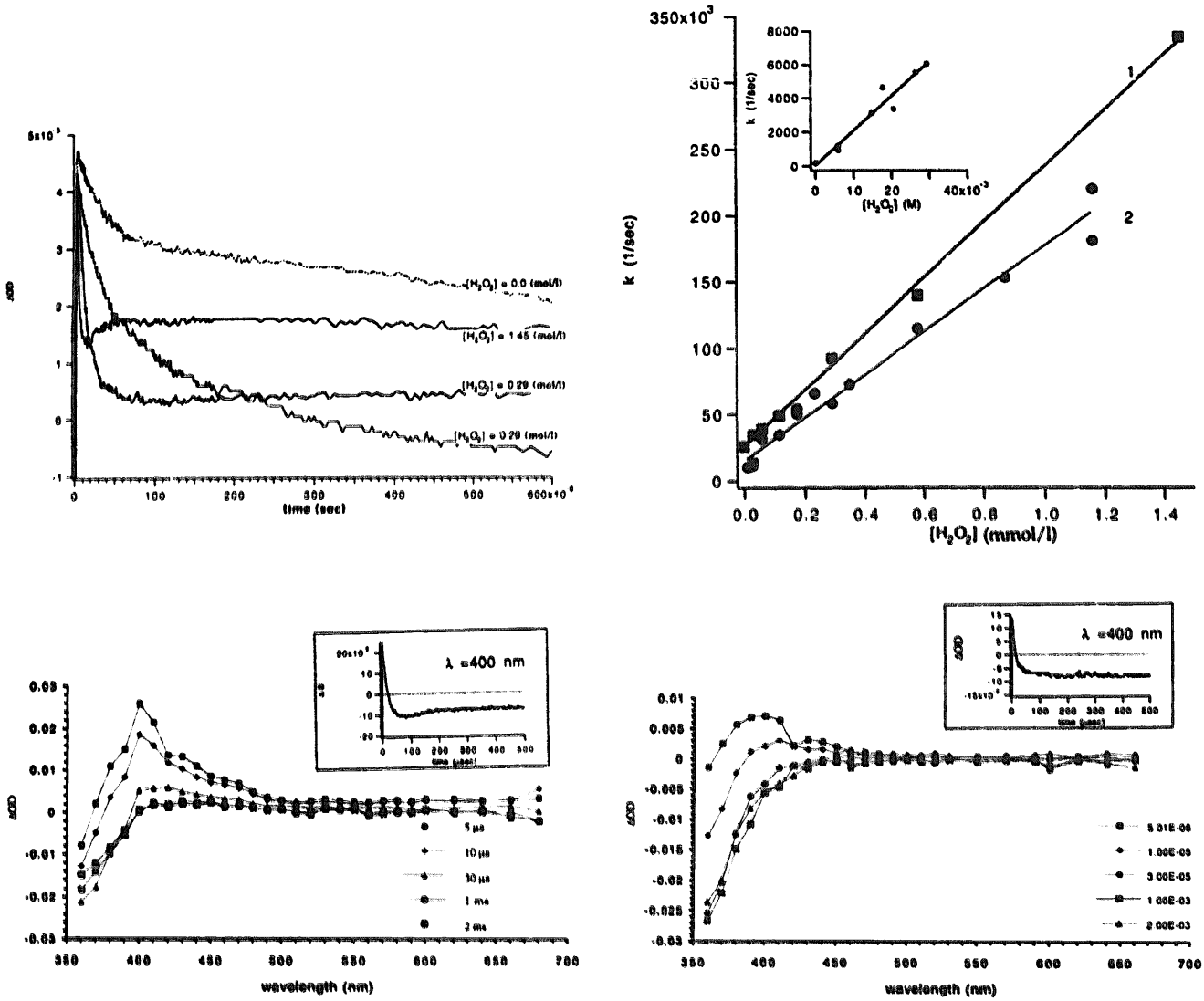

Fig. 5. (a) Differential optical density vs. time for a solution of Fe^{III} (0.6 mmol l^{-1}) and oxalate (18 mmol l^{-1}) at pH 6.5. The quenching concentrations of H_2O_2 used are noted. (b) Stern–Volmer rate constants for the reaction of $Fe(ox)_3^{3-}$* vs. H_2O_2 concentration using Fe^{III} (0.6 mmol l^{-1}) and oxalate (18 mmol l^{-1}) (circles) and Fe^{III} (0.6 mmol l^{-1}) and oxalate (1.2 mmol l^{-1}) (squares). The inset presents the slow component quenching by dilute H_2O_2 solution. (c) Transient spectra decay for a solution of Fe^{III} (0.6 mmol l^{-1}) and oxalate (18 mmol l^{-1}) at pH 6.6 in the presence of H_2O_2 (0.29 mol l^{-1}) at the times noted. At $\lambda = 400$ nm, the bleaching of the transient is shown as a function of time. (d) The same as in (c) but at pH 1.1.

Table 1
Rate constants for the quenching of $Fe(ox)_3^{3-}$* and $(ox)_2Fe(ox^{\cdot -})$ by H_2O_2

Substance	k ((mol l^{-1})$^{-1}$ s^{-1})	Conditions
$Fe(ox)_3^{3-}$* (fast component), ox = 18 mmol l^{-1}	$(2.1 \pm 0.1) \times 10^5$	pH 6.5, Fe^{III} = 0.6 mmol l^{-1}
$Fe(ox)_3^{3-}$* (fast component), ox = 1.2 mmol l^{-1}	$(1.6 \pm 0.1) \times 10^5$	pH 6.5, Fe^{III} = 0.6 mmol l^{-1}
$Fe(ox)_3^{3-}$* (fast component), ox = 18 mmol l^{-1}	$(6.1 \pm 0.1) \times 10^5$	pH 1.5, Fe^{III} = 0.6 mmol l^{-1}
$(ox)_2Fe(ox^{\cdot -})$ (slow component), ox = 18 mmol l^{-1}	$(2.0 \pm 0.2) \times 10^5$	pH 6.5, Fe^{III} = 0.6 mmol l^{-1}

Table 1 summarizes the quenching rate of $Fe(ox)_3^{3-}$* and $(ox)_2Fe(ox^{\cdot -})$ by H_2O_2. The possible pathways for the reaction of the iron complex with H_2O_2 are

$$Fe^{III}(ox)_3^{3-}* + H_2O_2 \longrightarrow [Fe^{III}(ox)_3^{3-} \cdots H_2O_2] \quad (13)$$

$$Fe^{III}(ox)_3^{3-}* + H_2O_2 \longrightarrow Fe^{III}(ox)_2^{1-} + {}^{\cdot}OH + OH^- + C_2O_4^{\cdot -} \quad (14)$$

$$Fe^{III}(ox)_3^{3-}* + H_2O_2 \longrightarrow [Fe^{II}(ox)_2 \cdot OH]^- + ox^{\cdot -} + OH^- \quad (15)$$

Because the metastable $(ox)_2Fe(ox^{\cdot -})$ is also quenched by H_2O_2, a reaction sequence similar to Eqs. (13)–(15) should also be considered for this intermediate. This has not been dealt with in detail in the present study.

3.5. $Fe(ox)_3^{3-}$-induced fast formation of hydroxylated products of phenol. Intermediate 'OH radical formation

The main goal of the experiments in this section of the paper was to look for the radical products formed during the quenching of excited $Fe(ox)_3^{3-}$* or $(ox)_2Fe(ox^{\cdot -})$ by H_2O_2. The addition of suitable organic molecules, such as phenol, may provide the test for 'OH radical formation. Phenol was selected because of its small absorption on laser excitation at 347 nm, because the addition of the 'OH radical to phenol has been reported to be close to the diffusion limit (for phenol, this value is 1.4×10^{10} (mol $l^{-1})^{-1}$ s^{-1} [19]) and because the radical adducts formed during these reactions (or the products due to fast reactions) exhibit absorption in the visible allowing detection of the spectral Δ OD changes. The fast reactions observed in Fig. 6 for 'OH radicals with phenol lead to coloured products with similar rise times as the lifetimes of $Fe(ox)_3^{3-}$*. This species was seen in Fig. 5 to be quenched by H_2O_2. The production of 'OH radicals in the dark reaction between Fe^{II} and H_2O_2 should proceed on a timescale longer than 10 ms.

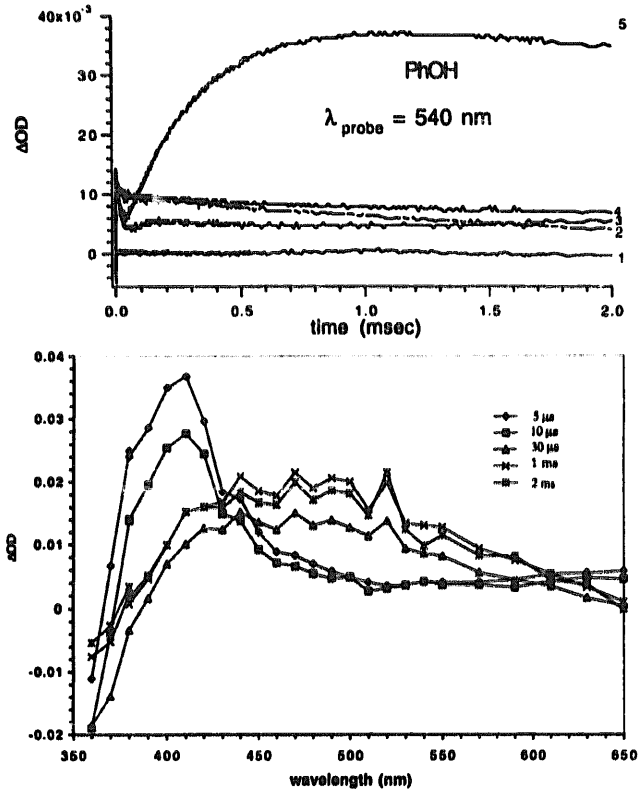

Fig. 6. (a) Laser-induced transients for: (1) a solution of phenol (79 mmol l^{-1}) and H_2O_2 (0.29 mol l^{-1}); (2) the same solution concentration of H_2O_2 and $Fe(ox)_3^{3-}$; (3) the decay of $Fe(ox)_3^{3-}$ (0.6 mmol l^{-1}) alone; (4) the decay of $Fe(ox)_3^{3-}$ in the presence of phenol (79 mmol l^{-1}); (5) the growth of the transient when the solution contains $Fe(ox)_3^{3-}$ (0.6 mmol l^{-1}), H_2O_2 (0.29 mol l^{-1}) and phenol (79 mmol l^{-1}). (b) Differential optical density of the transient decay as a function of λ when a solution similar to that used in (a) is employed at different times after the laser pulse (pH 6.5).

The characteristic lifetime for Fe^{II} from Eq. (16)

$$Fe^{II} + H_2O_2 \rightarrow Fe^{III} + OH^- + {}^{\cdot}OH$$

$$k_{16} = 41-75 \text{ (mol } l^{-1})^{-1} s^{-1} \quad (16)$$

can be estimated to be between 13 and 65 ms for H_2O_2 concentrations of 0.02–1.0 mol l^{-1}. If we estimate the lifetime for the species intervening in reaction (16) [6], this value is about 10^3 larger than when the photolysis is carried out via $Fe(ox)_3^{3-}$. Therefore the Fe complex reacts much faster with the oxidant than the classical Fenton reagent. The species $Fe(ox)_3^{3-}$* will react in the presence of H_2O_2 as suggested in Eqs. (15) and (16). For simplicity of presentation, the reaction routes involving $Fe^{IV}O$ and $(Fe\text{–}H_2O_2)$ complexes, recently suggested [16,17], have not been considered.

Fig. 6(a) presents the transient species after the laser pulse for: (1) phenol (79 mmol l^{-1}) added to H_2O_2 (0.29 mol l^{-1}) (no reaction); (2) $Fe(ox)_3^{3-}$ (0.6 mmol l^{-1}) reacting with H_2O_2 (0.29 mol l^{-1}); (3) the decay transient for $Fe(ox)_3^{3-}$ (0.6 mmol l^{-1}); (4) the decay of $Fe(ox)_3^{3-}$ in the presence of phenol (79 mmol l^{-1}) showing the small quenching effect of the latter; (5) the complete system $Fe(ox)_3^{3-}$ (0.6 mmol l^{-1}), H_2O_2 (0.29 mol l^{-1}) and phenol (79 mmol l^{-1}). The quenching of the initial Fe oxalate excited state is followed by the growth of a new band in the visible region due to the hydroxylated products of phenol [19]. The additional absorbance after the laser pulse in the system $Fe(ox)_3^{3-}$–H_2O_2–phenol is due to the development of coloured products. This reaction is two orders of magnitude faster than that expected for the Fenton dark reaction as previously mentioned. Therefore we assume that quenching of the Fe oxalate complex in the presence of peroxides produces strong oxidative 'OH radicals.

Fig. 6(b) shows the differential spectra for the system $Fe(ox)_3^{3-}$–H_2O_2–phenol. The transient decays at 360, 400 and 500 nm were observed to be different, showing that different species are formed during the decay. These species involve different radicals, adduct formation and a mixture of dihydroxylated products of phenol [19]. Fig. 6(b) presents the optical density of coloured product formation after the laser pulse when the Fe oxalate complex, phenol and H_2O_2 are reacted together in solution. The 'OH radicals formed during the interaction of Fe oxalate and H_2O_2 participate in competitive reactions during phenol hydroxylation

$$\text{phenol} + {}^{\cdot}OH \rightarrow \text{phenol}- -OH(\text{adduct})$$

$$k_{17} = 1.4\times10^{10} \text{ (mol } l^{-1})^{-1} s^{-1} \quad (17)$$

$$H_2O_2 + {}^{\cdot}OH \rightarrow HO_2^{\cdot} + H_2O$$

$$k_{18} = 1.3\times10^{7} \text{ (mol } l^{-1})^{-1} s^{-1} \quad (18)$$

$$ox^{2-} + {}^{\cdot}OH \rightarrow OH^- + ox^{\cdot -}$$

$$k_{19} = 2\times10^{6} \text{ (mol } l^{-1})^{-1} s^{-1} \quad (19)$$

$$^{\bullet}OH + {}^{\bullet}OH \rightarrow H_2O_2$$

$$k_{20} = 5.3 \times 10^9 \ (\text{mol l}^{-1})^{-1}\,\text{s}^{-1} \qquad (20)$$

$$^{\bullet}OH + Fe^{II} \rightarrow OH^- + Fe^{III}$$

$$k_{21} = 3 \times 10^8 \ (\text{mol l}^{-1})^{-1}\,\text{s}^{-1} \qquad (21)$$

Under the experimental conditions used $[H_2O_2] \gg [Fe^{II}]$, $[H_2O_2] \gg [ox^{2-}]$ and $[H_2O_2] \gg [^{\bullet}OH]$. In agreement with Eqs. (17) and (18) and Eqs. (2)–(5), a system of differential equations can be solved for the colour formation as a function of time

$$d[Fe(ox)_3^{3-}*]/dt = -k_q[Fe(ox)_3^{3-}*] - k_a[H_2O_2][Fe(ox)_3^{3-}*] \qquad (22)$$

$$d[^{\bullet}OH]/dt = k_{14}[H_2O_2][Fe(ox)_3^{3-}*] - k_{18}[^{\bullet}OH][H_2O_2] - k_{17}[^{\bullet}OH][\text{phenol}] \qquad (23)$$

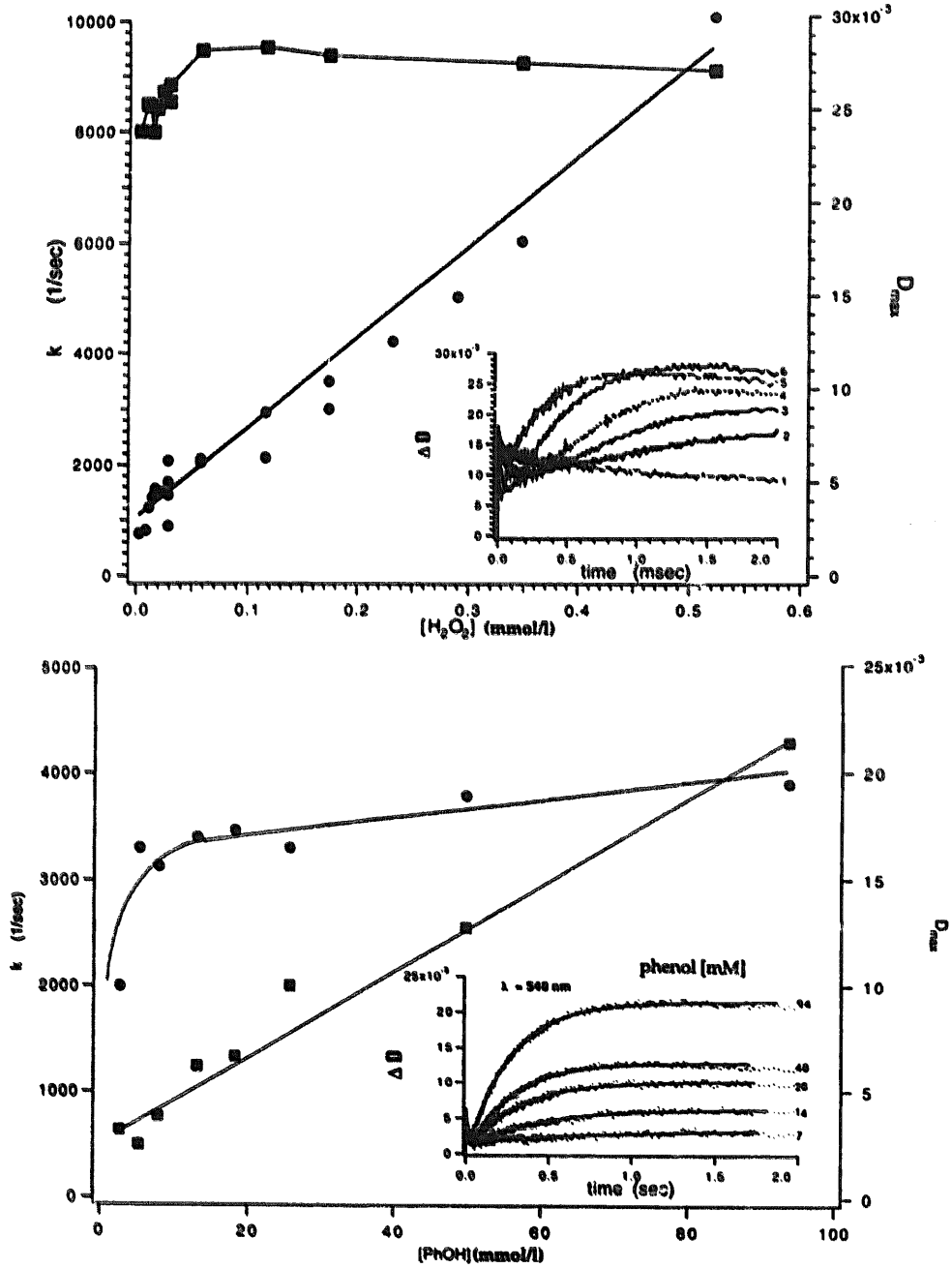

Fig. 7. (a) Dependence of the reciprocal rise time of the phenol adducts on the H_2O_2 concentration (circles). $Fe(ox)_3^{3-}$ (Fe^{III} (0.6 mmol l^{-1}) and oxalate (18 mmol l^{-1})) and phenol (79 mmol l^{-1}). Plot of the maximum optical density (D_{max}) vs. H_2O_2 concentration (squares). The inset shows the transient at $\lambda = 450$ nm when H_2O_2 is added at the following concentrations (mol l^{-1}): (1) 0.005; (2) 0.03; (3) 0.1; (4) 0.16; (5) 0.43; (6) 0.57. (b) Dependence of the reciprocal rise time of the phenol adducts (squares) and D_{max} (circles) on the phenol concentration. The inset shows the transients obtained at certain phenol concentrations at $\lambda = 450$ nm. The full lines show the fitting obtained by modelling the experimental points using Eq. (25).

$$d[\text{adduct}]/dt = k_{17}[{}^{\cdot}OH][\text{phenol}] \quad (24)$$

Since $k_{18}[H_2O_2] \gg k_a[H_2O_2]$

$$\Delta OD(t) = D_{max} - \text{cte} \exp(-k_q + k_a[H_2O_2])t \quad (25)$$

where the terms D_{max}, k_a and cte are

$$D_{max} = k_8 k_a [H_2O_2][\text{phenol}][Fe(ox)_3^{3-}*]/$$
$$[(k_q + k_a[H_2O_2])(k_{18}[H_2O_2] + k_{17}[\text{phenol}])]$$

$$k_a = k_{13} + k_{14} + k_{15}$$

and

$$\text{cte} = k_{17}k_{14}[H_2O_2][\text{phenol}][Fe(ox)_3^{3-}*]/(k_{18}[H_2O_2] + k_{17}[\text{phenol}] - k_q + k_2[H_2O_2])$$

Fig. 7(a) and 7(b) present the dependence of the reciprocal rise time k (s^{-1}) and maximum amplitude of the coloured product D_{max} as a function of H_2O_2 and phenol concentration. The rate constant observed for colour formation vs. H_2O_2 is $(1.6 \pm 0.1) \times 10^5$ $(\text{mol l}^{-1})^{-1}\,s^{-1}$ under the following experimental conditions: pH 6.5, $Fe^{III} = 0.6$ mmol l^{-1}, oxalate = 18 mmol l^{-1}, phenol concentration = 79 mmol l^{-1}.

The insert shows the transient decay at different H_2O_2 concentrations. The value of k is proportional to the H_2O_2 concentration in Fig. 7(a). It is nearly independent of the phenol concentration as shown in Fig. 7(b). These experimental results confirm the prediction stated in Eq. (22). The slope in Fig. 7(a) has a value of $(1.6 \pm 0.2) \times 10^5$ $(\text{mol l}^{-1})^{-1}\,s^{-1}$. This value is close to the rate constant observed for the quenching of the excited states of ferrioxalate and confirms the kinetic scheme outlined in Eqs. (17)–(21) for the $^{\cdot}OH$ radical reactions.

The experimental observations of adduct formation in Fig. 7 and the amplitude of D_{max} as a function of the H_2O_2 concentration fit well with the results obtained from Eq. (22). If we assume $k_q(Fe^{III}(ox)_3^{3-}*) \approx 32 \times 10^3\ s^{-1}$ in Eq. (9), the calculated values for D_{max} vs. H_2O_2 using the rate constants of Eqs. (17) and (18) should significantly increase up to $H_2O_2 = 1$ mol l^{-1}. This does not entirely agree with the experimental results reported in Fig. 7(a). Assuming that $k_q = 2.5\ ms^{-1}$ is the reciprocal lifetime of $(ox)_2Fe(ox^{\cdot -})$, the predicted dependence of D_{max} on H_2O_2 is observed to be close to the experimental value. The quenching of $(ox)_2Fe(ox^{\cdot -})$ (Eq. (5)) by H_2O_2 will proceed preferentially via $^{\cdot}OH$ radicals and not through $Fe(ox)_3^{3-}*$ LMCT deactivation due to H_2O_2 as outlined previously in Eqs. (13) and (15).

4. Conclusions

In this report, the fast kinetics of $Fe(ox)_3^{3-}$ decay and its quenching by H_2O_2 have been explored. The basic features of the light-driven excited states and certain redox reactions in homogeneous solutions are presented. The transient spectroscopy involved in phenol–OH adduct formation in the Fe oxalate–phenol–H_2O_2–UV system has been reported in detail. The implications of these observations for the light-driven degradation of pollutants when iron complexes are added have been elaborated. It seems that $^{\cdot}OH$ radical species are formed in fast reactions in the presence of light. The oxalate complexes provide adequate fast routes for adduct formation between phenol and H_2O_2. This is important in industrial-type pollution. From the pH experiments reported in Table 1 for the $Fe(ox)_3^{3-}$–H_2O_2 reaction, Fe^{III} interacts faster with H_2O_2 in acidic media and at a slower rate at pH > 3–4. Therefore only protonated systems seem to react efficiently with H_2O_2 in the presence of the strong oxidizing couple Fe^{III}/Fe^{II} (0.77 V). Since the Fe oxalate system absorbs far into the visible, the potential exists for its use in solar-induced degradations.

Acknowledgements

This work was supported by grant no. EV5V-CT9-0249 from the Commission of Economic Communities (OFES contract no. 95 00 31, Bern) and through the INTAS Cooperation Project Brussels no. 094-642.

References

[1] G. Helz, R. Zepp and D. Crosby (eds.), *Aquatic and Surface Chemistry*, CRC Press, Boca Raton, FL, 1990.
[2] Ch. Walling and R. Johnson, *Acc. Chem. Res., 8* (1975) 125.
[3] M. Hoffmann, S. Martin, W. Choi and D. Bahnemann, *Chem. Rev., 95* (1995) 69.
[4] J. Bolton, *Adv. Oxid. Technol., 1* (1996) in press.
[5] J. Kiwi and M. Gratzel, *J. Phys. Chem., 84* (1980) 1503.
[6] V. Balzani and V. Carassiti, in *Photochemistry of Coordination Compounds*, Academic Press, London, New York, 1970.
[7] E. Moorehead and N. Sutin, *Inorg. Chem., 5* (1966) 1806.
[8] L. Sillen and A. Martell (eds.), *Stability Constants of Metal-Ion Complexes*, Suppl. 1, Special Publication No. 25, The Chemical Society, London, 1971, p. 246.
[9] G. Cooper and B. DeGraff, *J. Phys. Chem., 75* (1971) 2897.
[10] Y. Zuo and J. Hoigné, *Environ. Sci. Technol., 26* (1992) 1014.
[11] Y. Zuo and J. Hoigné, *Atmos. Environ., 28* (1994) 1231.
[12] C. Hatchard and C. Parker, *Proc. R. Soc. London, Ser. A, 235* (1956) 518.
[13] D. Cooper and B. DeGraff, *J. Phys. Chem., 76* (1972) 2618.
[14] S. Lunak and T. Siska, *Collect. Czech. Chem. Commun., 48* (1983) 3033.
[15] R. Zepp, B. Faust and J. Hoigné, *Environ. Sci. Technol., 26* (1992) 319.
[16] C. Sheu, A. Sobkowiak, L. Zhang, N. Ozbalik, D. Barton and D. Sawyer, *J. Am. Chem. Soc., 11* (1989) 8030.
[17] D. Sawyer, K. Chang, A. Llobet and Ch. Redman, *J. Am. Chem. Soc., 115* (1993) 5817.
[18] J. Pignatello, *Environ. Sci. Technol., 26* (1992) 1014.
[19] E. Land and M. Ebert, *Trans. Faraday Soc., 63* (1967) 1181.